

Suppression of HD–cooling in protogalactic gas clouds by Lyman–Werner radiation

J. Wolcott-Green^{1*} and Z. Haiman^{2*}

¹*Barnard College, Columbia University, 3009 Broadway, New York, NY 10027*

²*Department of Astronomy, Columbia University, 550 West 120th Street, New York, NY 10027*

ABSTRACT

It has been shown that HD molecules can form efficiently in metal-free gas collapsing into massive protogalactic halos at high redshift. The resulting radiative cooling by HD can lower the gas temperature to that of the cosmic microwave background, $T_{\text{CMB}} = 2.7(1+z)\text{K}$, significantly below the temperature of a few $\times 100\text{K}$ achievable via H_2 –cooling alone, and thus reduce the masses of the first generation of stars. Here we consider the suppression of HD–cooling by UV irradiation in the Lyman–Werner (LW) bands. We include photo-dissociation of both H_2 and HD, and explicitly compute the self-shielding and shielding of both molecules by neutral hydrogen, HI, as well as the shielding of HD by H_2 . We use a simplified dynamical collapse model, and follow the chemical and thermal evolution of the gas, in the presence of a UV background. We find that a LW flux of $J_{\text{crit,HD}} \approx 10^{-22} \text{erg cm}^{-2} \text{sr}^{-1} \text{s}^{-1} \text{Hz}^{-1}$ is able to suppress HD cooling and thus prevent collapsing primordial gas from reaching temperatures below $\sim 100\text{K}$. The main reason for the lack of HD cooling for $J > J_{\text{crit,HD}}$ is the partial photo-dissociation of H_2 , which prevents the gas from reaching sufficiently low temperatures ($T < 150\text{K}$) for HD to become the dominant coolant; direct HD photo-dissociation is unimportant except for a narrow range of fluxes and column densities. Since the prevention of HD–cooling requires only partial H_2 photo-dissociation, the critical flux $J_{\text{crit,HD}}$ is modest, and is below the UV background required to reionize the universe at $z \sim 10 - 20$. We conclude that HD–cooling can reduce the masses of typical stars only in rare halos forming well before the epoch of reionization.

Key words: cosmology: theory – early universe – galaxies: formation – molecular processes

1 INTRODUCTION

The first generation of stars are believed to be much more massive ($\sim 100M_{\odot}$) than typical stars in stellar populations in the low-redshift universe ($\sim 1M_{\odot}$; Bromm et al. 2002; Abel et al. 2002). This has many important consequences in the early universe, for reionization, metal-enrichment, the formation of seed black holes at very early times, and the observability of first-generation galaxies.

The high masses result from the thermodynamical properties of H_2 , the main coolant in low-temperature gas with a primordial composition. In particular, H_2 –cooling becomes ineffective at temperatures below $\sim 200\text{K}$. HD molecules, can, in principle, cool the gas to much lower temperatures, but until recently, the abundance of HD in the early universe was believed to be too low for it to be important.

It has recently been pointed out that significant HD

can form in metal-free gas, due to non-equilibrium chemistry, provided that the gas has a large initial electron fraction. This can occur, for example, in “fossil” gas that was ionized by a short-lived massive star, prior to it being extinguished, or in collisionally-ionized halos with virial temperatures above $\approx 10^4\text{K}$. It has been shown that the resulting radiative cooling by HD can then lower the gas temperature to values near that of the cosmic microwave background, $T_{\text{CMB}} = 2.7(1+z)\text{K}$, i.e. to $\sim 30\text{K}$ at $z \sim 10$. This would decrease the expected masses of the stars that form in ionized halos by a factor of ~ 10 below that which is possible if HD-cooling is neglected (e.g. Johnson & Bromm 2006).¹ Thus, a second mode of star formation has been proposed, giving rise to Pop. III.2 stars² that can form

¹ Using three-dimensional simulations, McGreer & Bryan (2008) found that HD lowers the expected Pop. III masses less dramatically, but still has an important effect.

² Adopting the terminology suggested by Bromm et al. (2009).

* E-mail: jemma@astro.columbia.edu;
zoltan@astro.columbia.edu

as soon as a small number of Pop. III.1 stars have initiated the epoch of reionization, and whose masses are only a few tens of solar masses (Nakamura & Umemura 2002; Machida et al. 2005; Nagakura & Omukai 2005; Johnson & Bromm 2006; Ripamonti 2007; Yoshida et al. 2007a; Yoshida et al. 2007b).

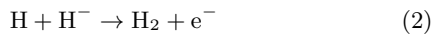
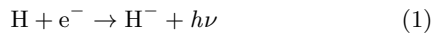
These conclusions could potentially be revised, however, due to the suppression of HD-cooling by UV irradiation of the gas cloud. Although this possibility has been raised in the literature (e.g. Johnson & Bromm 2006; Yoshida et al. 2007b), previous work has not included a detailed treatment of the impact of UV irradiation on HD-cooling, including photo-dissociation of HD by radiation in its Lyman and Werner (hereafter LW) bands, taking into account the shielding that occurs in the optically thick regimes. Such UV radiation will exist in the early universe, and can suppress H₂-cooling in low-mass halos at high redshifts (e.g., Haiman et al. 1997). *The main goal of this paper is to assess whether HD-cooling can be similarly suppressed by UV radiation, and to compute the critical UV flux for the HD-destruction.*

In order to do this, we perform “one zone” calculations with a simplified density evolution, while following the gas-phase chemistry and thermal evolution of the gas, including the impact of H₂- and HD-dissociating LW radiation. In general, collapsing gas clouds become optically thick to this radiation, so that the effects of self-shielding are non-negligible. Our treatment includes self-shielding of HD and H₂, shielding of both species by neutral hydrogen (HI), and shielding of HD by H₂. We provide useful fitting formulae for these shielding factors, analogous to the case of H₂ self-shielding studied by Draine & Bertoldi (1996) (hereafter DB96).

The rest of this paper is organized as follows. In § 2 we describe our chemical, thermal, and dynamical modeling. § 3 presents our results on the critical flux required to suppress HD-cooling, followed by a brief discussion of the potential cosmological implications and primary uncertainties in § 4. We summarize our main results and offer our conclusions in § 5. Throughout this paper, we adopt the standard Λ CDM cosmological background model, with the following parameters: $\Omega_{\text{DM}} = 0.233$, $\Omega_{\text{b}} = 0.0462$, $\Omega_{\Lambda} = 0.721$, and $h = 0.701$ (Komatsu et al. 2009).

2 MODEL DESCRIPTION

The formation of HD occurs primarily through the following reaction sequence (e.g. Galli & Palla 2002):



Thus, in order to form a significant abundance of HD, a large initial electron fraction is required to catalyze the formation of H₂ (see, e.g. Johnson & Bromm 2006, and references therein). In primordial gas this can be achieved by photoionization (e.g. by short-lived Pop III.1 stars), or by collisional ionization (in sufficiently massive halos). We model the first case by a constant, low-density gas, initially at a density

comparable that of the intergalactic medium (IGM) at high redshift, $n \approx 10^{-7}(1+z)^3 \text{ cm}^{-3}$, and temperature $T \approx 10^4 \text{ K}$. We model the second case by a pre-imposed density evolution obtained from the spherical collapse model.

2.1 One-Zone Spherical Collapse Model

We adopt the model for homologous spherical collapse that has been used in several previous studies (e.g. Omukai et al. 2008; hereafter OSH08). This simple one-zone treatment prescribes the density evolution of the baryonic and dark matter (DM) components of a collapsing halo. Both are initialized with zero velocity at the turnaround redshift, set throughout this paper to $z = 17$. The density of the infalling gas evolves on the free-fall timescale and that of the DM is given by a top-hat overdensity until virialization, after which it remains constant at its virial value. Compressional heating is included in the thermal model, along with the processes listed in § 2.2.

Unless stated otherwise, we take the radius of the cloud to be $R_{\text{c}} = \lambda_{\text{J}}/2$, where the Jeans length is given by

$$\lambda_{\text{J}} = \sqrt{\frac{\pi k_{\text{B}} T_{\text{gas}}}{G \rho_{\text{gas}} \mu m_{\text{p}}}}, \quad (4)$$

Here k_{B} is Boltzmann’s constant, T_{gas} is the gas temperature, μ is the mean molecular weight, and m_{p} is the mass of the proton. Note that the size of the cloud is required, in practice, only in our calculations of the self-shielding factors (see below), in order to specify the column densities of H₂, HD, and HI.

While this model is a vast simplification of the physics of a collapsing halo, it nonetheless has been shown to mimic the thermal and chemical evolution seen in full three-dimensional hydrodynamical simulations very well (see, e.g., Shang et al. 2010 – hereafter SBH10 – for a direct comparison). The exception is the shock-heating that occurs in the early stages of collapse and is not present in the one-zone model, which prescribes a smooth “free-fall” evolution. For a detailed description of the spherical collapse model, the reader is referred to the recent work by OSH08 and references therein.

2.2 Chemical and Thermal Model

We model a gas of primordial composition using a reaction network which comprises 47 gas-phase reactions amongst the following 14 chemical species (and photons): H, H⁺, H[−], He, He⁺, He²⁺, H₂, H₂⁺, D, D⁺, D[−], HD, HD⁺, and electrons. Our choices for the selection of species and their initial abundances are conventional (see, e.g., Galli & Palla 1998), but we do not include any lithium species or other potential coolants (e.g. H₃⁺), as they contribute very little to the total cooling (e.g. Glover & Savin 2009) and are not important in the context of this paper.

2.2.1 Hydrogen and Helium Chemistry

The collisional rate coefficients for reactions among hydrogen and helium species only, and cross-sections for photoionization, are taken from the recent compilation by SBH10.

However, the rate for H_2 photo-dissociation (k_{28} in the aforementioned compilation) is modified to $k_{\text{diss},\text{H}_2} = 1.39 \times 10^{-12} \times \beta \times f_{\text{shield}}$ in order to match the optically thin rate we calculate (see § 2.3). The total shielding is parameterized by a shield factor, f_{shield} (see below), and the rate is normalized by the parameter β , as described by in Appendix A of OM01, which specifies the intensity of blackbody radiation at the average LW band energy (12.4 eV) relative to that at the Lyman limit (13.6 eV). For the two spectral types we consider (described in § 3), $\beta = 3$ for the T4-type and $\beta = 0.9$ for the T5-type.

2.2.2 Deuterium Chemistry

The chemical network includes 19 reactions involving the five deuterium species, for which we use the collisional rate coefficients from the compilation by Nakamura & Umemura (2002). However, we replace the rates D2, D3, D7, and D9 given therein (as referenced in the source) with the corresponding updated rates from Savin (2002) (for the charge exchange reactions, D2 and D3) and Galli & Palla (2002) (for D7 and D9). The HD photo-dissociation rate is given in § 2.3 and is normalized with the β parameter in the same manner as described above for the H_2 photo-dissociation rate.

We take the cosmological D/H ratio to be 4×10^{-5} by number, following recent studies on HD-cooling (e.g. Johnson & Bromm 2006, Yoshida et al. 2007) and inspired by the model of Galli & Palla (1998), which provides a value of $\text{D}/\text{H} = 4.3 \times 10^{-5}$. This adopted value is likely overgenerous for the primordial deuterium abundance, however, in light of recent observations, which place estimates of D/H at $2.78^{+0.44}_{-0.38} \times 10^{-5}$ (Kirkman et al. 2003) and $2.82^{+0.27}_{-0.25} \times 10^{-5}$ (O’Meara et al. 2006). However, decreasing the initial deuterium abundance in our models leads to less robust HD-cooling, and so only serves to strengthen our central conclusion that metal-free gas is unlikely to be cooled, by HD, to temperatures close to T_{CMB} .

In § 4, we discuss recently updated rate coefficients for some of the most important reactions, and how their implementation affects our results.

2.2.3 Thermal Model

The following processes are included in the net cooling rate: collisional excitation and ionization (of H, He, and He^+), recombination (to H, He, and He^+), dielectric recombination (to He), Bremsstrahlung, Compton cooling,³ and molecular cooling by H_2 and HD. In practice, the last two processes, as well as collisional excitation of HI, dominate in our calculations. We adopt the expression provided by Galli & Palla (1998) for H_2 cooling. In the fossil gas case, the HD-cooling rate is calculated using the analytic fit for low densities ($n \lesssim 10^3 \text{ cm}^{-3}$) given by equation (5) in Lipovka et al. (2005). In the spherical collapse runs, we adopt the lengthier polynomial fit (equation 4 in the same source), which is accurate for gas densities $n \lesssim 10^8 \text{ cm}^{-3}$.

We note that T_{CMB} is a “temperature floor,” below

which gas cannot cool radiatively; if the gas temperature were below T_{CMB} , interaction with photons in the roto-vibrational bands would heat, rather than cool the gas. In order to mimic this behavior, we multiply Λ_{H_2} and Λ_{HD} by a correction factor $(T - T_{\text{CMB}}) / (T + T_{\text{CMB}})$. This ensures that cooling is shut-off as the temperature approaches T_{CMB} from above (whereas the correction becomes negligible when $T \gg T_{\text{CMB}}$; see Haiman et al. 1996 and Johnson & Bromm 2006 for a somewhat more accurate approach).

Our thermal model includes heating from photo-detachment of H^- , high energy electrons resulting from photo-ionization of helium (see, e.g., Appendix B in Haiman et al. 1996), as well as compressional heating in the model of adiabatic collapse (see OSH08 and references therein for more details). In practice, the latter dominates in the regime of our calculations.

In order to follow the coupled chemical and thermal evolution of the gas we use the Livermore solver LSODAR to solve the stiff equations.

2.3 HD and H_2 Photo-dissociation in the Optically Thin Limit

HD and H_2 can be dissociated by photons with energies in the range 11.2–13.6 eV, to which the universe is largely transparent even before the IGM is reionized. Although both HD and H_2 have LW lines above 13.6 eV, we do not include photons above this energy, because they will have been absorbed by neutral hydrogen elsewhere in the IGM prior to reionization. Here we describe the details of the calculation for HD photo-dissociation; however, the calculation for H_2 is entirely analogous, so the following applies equally well to both molecules.

Excitation of the HD molecule to its $B^1 \sum_u^+$ and $C^1 \Pi_u$ electronic states and subsequent radiative decay leads to dissociation when the system decays to the vibrational continuum of the ground state, rather than back to a bound state. Here we discuss the optically thin case, in which the processing of the LW spectrum by HD itself (as well as by H_2 and HI) is assumed to be negligible. The dissociation rate for molecules initially in the electronic ground state with vibrational and rotational quantum numbers (v, J) is given by:

$$k_{\text{diss},v,J} = \sum_{v',J'} \zeta_{v,J,v',J'} f_{\text{diss},v',J'} \quad (5)$$

where $f_{\text{diss},v',J'}$ is the dissociation probability from the excited state (v', J') and the pumping rate is given by

$$\zeta_{v,J,v',J'} = \int_{\nu_{th}}^{\infty} 4\pi\sigma_{\nu} \frac{J_{\nu}}{h_P\nu} d\nu. \quad (6)$$

Here σ_{ν} is the frequency-dependent cross-section of a given transition, h_P is Planck’s constant, and the specific intensity just below 13.6 eV is hereafter normalized as $J_{\nu} = J_{21} \times [10^{-21} \text{ erg cm}^{-2} \text{ sr}^{-1} \text{ s}^{-1} \text{ Hz}^{-1}]$. As mentioned above, in our model there is a sharp cut off in the radiation spectrum above 13.6 eV; the lower limit, ν_{th} , is the frequency threshold, corresponding to the longest-wavelength photons included, $\lambda \sim 1105 \text{ \AA}$.

In principle, the total dissociation rate also depends on the level populations of the molecule, which in turn depend on the incident radiation field as well as the temperature and

³ Numerical expressions for these cooling processes can be found in, e.g., Haiman et al. (1996).

density of the gas; thus, the total dissociation rate should be:

$$k_{\text{diss,tot}} = \sum_{v,J} k_{\text{diss},v,J} f_{v,J}, \quad (7)$$

where $f_{v,J}$ is the fraction of molecules initially in the ro-vibrational state denoted by v, J . For simplicity, we assume that all HD and H₂ molecules are initially in the ground state (i.e. $f_{v=0,J=0} = 1$). This is a reasonable approximation for low gas densities, at which the populations of higher ro-vibrational states are very small. However, the level populations of H₂ and HD reach their values at local thermodynamic equilibrium when gas densities rise to $n \gtrsim 10^4 \text{ cm}^{-3}$, and $n \gtrsim 10^6 \text{ cm}^{-3}$ respectively. In § 4, we discuss the differences in the dissociation rates if both molecules are assumed to be in LTE, and how this impacts the results discussed below.

We include 28 discrete spectral lines of HD and 25 of H₂, all involving transitions from the ground electronic state $X^1 \Sigma_g^+$ to the $B^1 \Sigma_u^+$ and $C^1 \Pi_u^+$ excited states. We use the necessary data for the Lyman and Werner bands of HD provided by Abgrall & Roueff (2006). For those of H₂, the relevant data were taken from Abgrall et al. (1993a), and Abgrall et al. (1993b). We use the updated dissociation fractions for H₂ in Abgrall et al. (2000). The numerical wavelength resolution in the calculations ($\Delta\lambda = 5.8 \times 10^{-5} \text{ \AA}$ at the lowest temperatures) is sufficient to resolve the Voigt profile of each line and explicitly account for overlap of the Lorentz wings. We find the following photo-dissociation rates in the optically thin limit: $k_{\text{diss,HD}} = 1.55 \times 10^9 J_\nu \text{ s}^{-1}$, and $k_{\text{diss,H}_2} = 1.39 \times 10^9 J_\nu \text{ s}^{-1}$, in excellent agreement with those found previously by Glover & Jappsen (2007): $k_{\text{diss,HD}} = 1.5 \times 10^9 J_\nu \text{ s}^{-1}$, and $k_{\text{diss,H}_2} = 1.38 \times 10^9 J_\nu \text{ s}^{-1}$. Here J_ν denotes the intensity at the average LW band of HD and H₂, with energy 12.4 eV, as discussed above.

2.4 Self-Shielding of HD and H₂

When sufficiently high column densities of HD or H₂ build up, ($N_{\text{HD}}, N_{\text{H}_2} \gtrsim 10^{13} \text{ cm}^{-2}$), the LW bands become optically thick and the rates of photo-dissociation are suppressed. We parameterize this effect by a shield factor, f_{shield} , akin to that given by DB96 in their study of H₂ self-shielding. In particular, $f_{\text{shield,HD}} \equiv k_{\text{diss,HD}}(N_{\text{HD}})/k_{\text{diss,HD}}(N_{\text{HD}} = 0)$ where $k_{\text{diss,HD}}(N_{\text{HD}} = 0)$ is the dissociation rate in the optically thin limit (equation 7), and the shield factor for H₂, $f_{\text{shield,H}_2}$, is analogously defined. Our treatment of H₂ self-shielding differs from the previous study by DB96 in that we assume all H₂ is in the ro-vibrational ground state (as described above), while the latter used a model allowing for populations in higher ro-vibrational levels due to collisional excitation and “UV pumping” by the incident radiation field. Nonetheless, we find that a good analytical fit for both H₂ and HD self-shielding is provided by the same functional form as equation (37) for $f_{\text{shield,H}_2}$ in DB96. We also find that the self-shielding behavior of the two molecules is nearly identical, (see Figure 1), which might be expected on the basis of

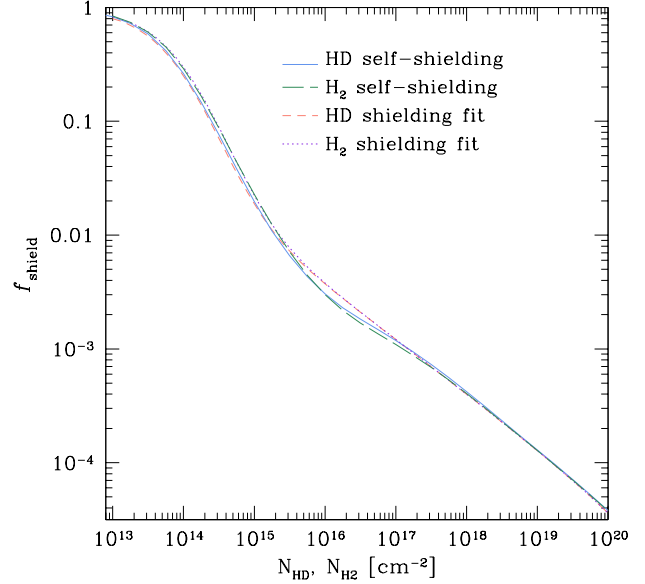


Figure 1. Solid (blue) and broken (green) curves show the numerically calculated self-shielding factors for HD and H₂ respectively; these are defined as the ratio of the dissociation rate at a given column density and the optically thin dissociation rate, and are shown as functions of the respective column densities. Dashed (orange) and dotted (magenta) curves show the values obtained by using the fitting formulae from equation 8 for HD and H₂ self-shielding, respectively (the slight difference here arises only because of the different masses of the two molecules, which modifies the Doppler parameter). All are shown at $T = 200 \text{ K}$.

the similarity in their electronic structures⁴; thus, we use the following fitting formula for both $f_{\text{shield,H}_2}(N_{\text{H}_2}, T)$ and $f_{\text{shield,HD}}(N_{\text{HD}}, T)$:

$$f_{\text{shield}}(N, T) = \frac{0.9379}{(1 + x/D_5)^{1.879}} + \frac{0.03465}{(1 + x)^{0.473}} \times \exp[-2.293 \times 10^{-4} (1 + x)^{0.5}], \quad (8)$$

where $x \equiv N/8.465 \times 10^{13} \text{ cm}^{-2}$, N is the column density of the self-shielding species, $D_5 \equiv b_D/10^5 \text{ cm s}^{-1}$, and the Doppler broadening parameter, b_D , depends on the mass of the molecule (which accounts for the slight difference in the self-shielding formula for the two molecules), as well as the temperature.

2.5 Shielding by HI and Mutual Shielding of H₂ and HD

In addition to self-shielding, HD and H₂ can also shield each other, and both can be shielded by HI, which has absorption lines in the range 11.2–13.6 eV; thus, suppression of the photo-dissociation rates depend on the relative strengths and positions of the HD, H₂, and HI lines, as well as the column densities of each species, N_{HD} , N_{H_2} , and N_{HI} .

⁴ The similarities in the line strengths of H₂ and HD, quantified by the product of the oscillator strength and dissociation fraction, can be seen in Figure 2 below.

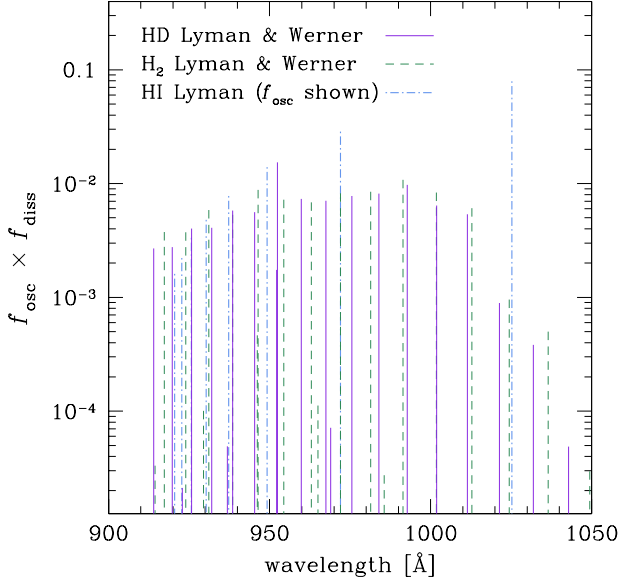


Figure 2. The figure illustrates the wavelengths and strengths of the relevant LW lines of H_2 and HD, as well as the Lyman series of HI. The solid (purple) and dashed (green) lines indicate the product of the oscillator strength and dissociation fraction for HD and H_2 respectively, drawn at the position of each line center. The wavelengths and oscillator strengths of the hydrogen Lyman series are similarly shown by the blue dash-dot lines (a dissociation fraction in this case is not applicable). At high HI column densities, the HD lines that dominate the dissociation rate are those at ~ 960 , ~ 980 , and ~ 990 Å, and the dominant contributions to the H_2 -dissociation rate are made by the absorption lines at ~ 945 , ~ 980 , and ~ 990 Å.

We include the first nine Lyman HI lines in the relevant wavelength range; while the line center of the Ly α line is outside this range, we nevertheless include it, as its contribution to the shielding becomes important due to line broadening at high HI column densities. For illustration, in Figure 2 we show the positions and strengths of the most significant lines of each species.

2.5.1 Shielding of HD by H_2 and HI

Taking shielding into account, the contribution to the HD-dissociation rate for a particular line at frequency ν becomes:

$$k_{\text{diss,HD},\nu}(N_{\text{HD}}) = k_{\text{diss,HD},\nu}(N_{\text{HD}} = 0) \exp(-\tau_{\nu}), \quad (9)$$

where the optical depth is given by

$$\tau_{\nu} = \sigma_{\text{HD},\nu} N_{\text{HD}} + \sigma_{\text{HI},\nu} N_{\text{HI}} + \sigma_{\text{H}_2,\nu} N_{\text{H}_2}. \quad (10)$$

While HD self-shielding becomes important for $N_{\text{HD}} \gtrsim 10^{13} \text{ cm}^{-2}$, the offsets in the wavelength of the neighboring absorption lines (typically of order $\sim \text{\AA}$) prevent H_2 and HI from effectively shielding HD until their column densities are very high, $N_{\text{H}_2} \gtrsim 10^{20} \text{ cm}^{-2}$, and $N_{\text{HI}} \gtrsim 10^{23} \text{ cm}^{-2}$. At these critical densities, which are essentially independent of N_{HD} , the H_2 lines start to significantly overlap and the optical depth due to H_2 -shielding is \sim a few at all wavelengths. In Figure 3, we show the evolution of all three column densities, as a function of the particle number density, in our

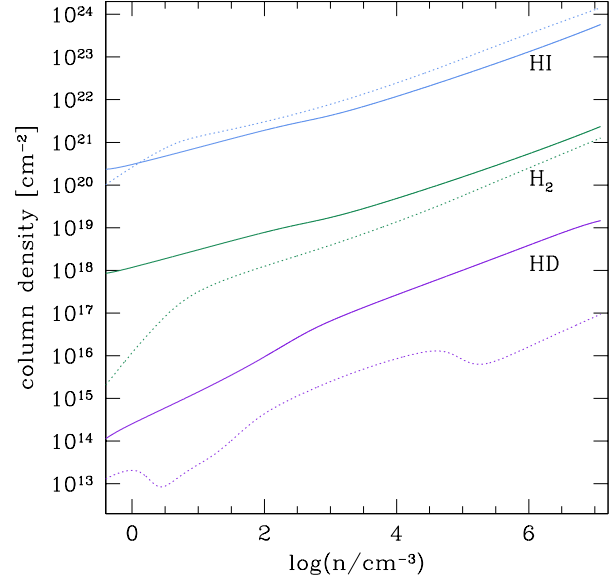


Figure 3. Column densities reached in the spherical collapse runs for halos with virial temperatures above and below 10^4 K , shown by solid and dotted lines respectively. Both runs assume no background flux ($J = 0$).

Table 1. Coefficients for the fitting formula for $f_{\text{shield,HD}}(N_{\text{HD}}, N_{\text{H}_2}, N_{\text{HI}}, T)$, representing the total combined shielding factor of HD, including shielding by H_2 and HI (equations 11 and 12). The analytic fit for self-shielding is given in equation 8.

Species	α	β	$\gamma \text{ (cm}^{-2}\text{)}$
1. HI	1.620	0.149	2.848×10^{23}
2. H_2	0.238	0.00520	2.339×10^{19}

one-zone collapse runs with $J = 0$ for halos with virial temperatures both above and below 10^4 K (see below). This figure shows that all three column densities reach the values where shielding becomes efficient, and thus a full calculation of the combined self-shielding is warranted.

We provide a fitting formula to model the total shielding of HD, $f_{\text{shield,HD}} = f_{\text{shield,HD}}(N_{\text{HD}}, N_{\text{H}_2}, N_{\text{HI}}, T)$ in Table 1 and equations 11, and 12 below, which is accurate to within a factor of two over a wide range of column densities, i.e. up to $N_{\text{HD}} \approx 10^{20} \text{ cm}^{-2}$, $N_{\text{H}_2} \approx 10^{22} \text{ cm}^{-2}$, $N_{\text{HI}} \approx 10^{24} \text{ cm}^{-2}$ and gas temperatures up to $\approx 10^3 \text{ K}$ (HD-cooling is unimportant at temperatures above this value in any case):

$$f_{\text{shield,HD}} = f_{\text{shield}}(N_{\text{HD}}, T) \times f_1(N_{\text{HI}}) \times f_2(N_{\text{H}_2}) \quad (11)$$

$$f_i = \frac{1}{(1 + x_i)^{\alpha_i}} \times \exp(-\beta_i x_i). \quad (12)$$

Here $x_i \equiv N_i/\gamma_i$ and the index i takes the value $i = 1$ or 2 to denote the relevant quantity for HI or H_2 respectively. The coefficients α , β , and γ are given in Table 1.

This fit is described by a product of three separate functions, $f_{\text{shield,HD}}(N_{\text{HD}}, T)$, $f_{\text{shield,H}_2}(N_{\text{H}_2})$, and

$f_{\text{shield,HI}}(N_{\text{HI}})$, which represent the shielding of HD due to each of the three species alone (eq. 11 above). Note that since the H_2 and HI lines shield HD by their Lorentz wings, rather than their thermal cores, these factors (unlike HD self-shielding) do not depend on temperature.

In general, one does not expect that the combined shielding factor is separable into a simple product of the three individual shielding factors. The full expression for $f_{\text{shield,HD}}(N_{\text{HD}}, N_{\text{H}_2}, N_{\text{HI}}, T)$ is a sum over all of the individual cross-sections of the HD lines, each suppressed by the frequency-dependent total optical depth (eq. 10), divided by the optically thin rate. However, we have found that in practice, when suppression by nearby HI lines is negligible ($N_{\text{HI}} \lesssim 10^{23} \text{ cm}^{-2}$), one HD line is much stronger than all others (at $\approx 950 \text{ \AA}$, see Figure 2). Since this single line dominates the dissociation rate, the shield factor reduces to the simple product (eq. 11 above). In the regime of relatively strong HI shielding ($N_{\text{HI}} \approx 10^{24} \text{ cm}^{-2}$), a few HD Lyman lines together dominate the dissociation rate. However, we find that the product $\sigma_\lambda \times f_{\text{diss},\lambda}$ for these lines (at ~ 960 , ~ 980 , and $\sim 990 \text{ \AA}$) are similar. If we approximate that these lines have identical strengths, the total shielding factor again reduces to the simple product in equation 11 above. Because these line strengths are not precisely equal, the largest discrepancies in the product formula and ‘true’ shielding behavior are seen at $N_{\text{HI}} = 10^{24} \text{ cm}^{-2}$. However, in general, we find that this simple product is accurate, to within a factor of \sim two, at the low temperatures ($T \lesssim 200 \text{ K}$) and the high column densities of interest.

Figure 4 shows the results of the exact shielding factor calculations for a gas temperature of $T = 200 \text{ K}$, and compares these to the analytical fits for a number of combinations of the three column densities. The largest deviations are seen in the bottom panel, for $N_{\text{HI}} = 10^{24} \text{ cm}^{-2}$, and at H_2 and HD column densities of $N_{\text{H}_2} = 10^{22} \text{ cm}^{-2}$ and $10^{14} \text{ cm}^{-2} \lesssim N_{\text{HD}} \lesssim 10^{15.5} \text{ cm}^{-2}$. In this regime, the accuracy of the fitting formulae is somewhat worse than a factor of two. However, in practice, this column density combination – with relatively low N_{HD} and exceedingly high values of both N_{H_2} and N_{HI} – does not occur in our calculations (see Figure 3).

2.5.2 Shielding of H_2 by HI and HD

The shielding of H_2 by HD and HI is entirely analogous to that discussed in the preceding section, so we will limit the discussion here to a few noteworthy points. Most importantly, we find that HI shielding of H_2 is nearly identical to HI shielding of HD; accordingly, we model both with the fitting formula for $f_{\text{shield,HI}}(N_{\text{HI}})$, given by equation 12 and Table 1. The explanation for this is similar to that given above; namely, the relative positions of the H_2 and HI lines is such that only the wings of the HI lines shield H_2 when the column densities of N_{HI} are sufficiently large ($N_{\text{HI}} \gtrsim 10^{23}$). Because the H_2 and HD lines are comparably spaced relative to the HI lines, the shielding effect of HI should indeed be similar for both.

When the HI column is below the critical level for strong shielding of H_2 , we find that a few Lyman lines together dominate the dissociation rate, and that the product $\sigma_\lambda \times f_{\text{diss},\lambda}$ for these lines (at ~ 945 , ~ 980 , and $\sim 990 \text{ \AA}$) are

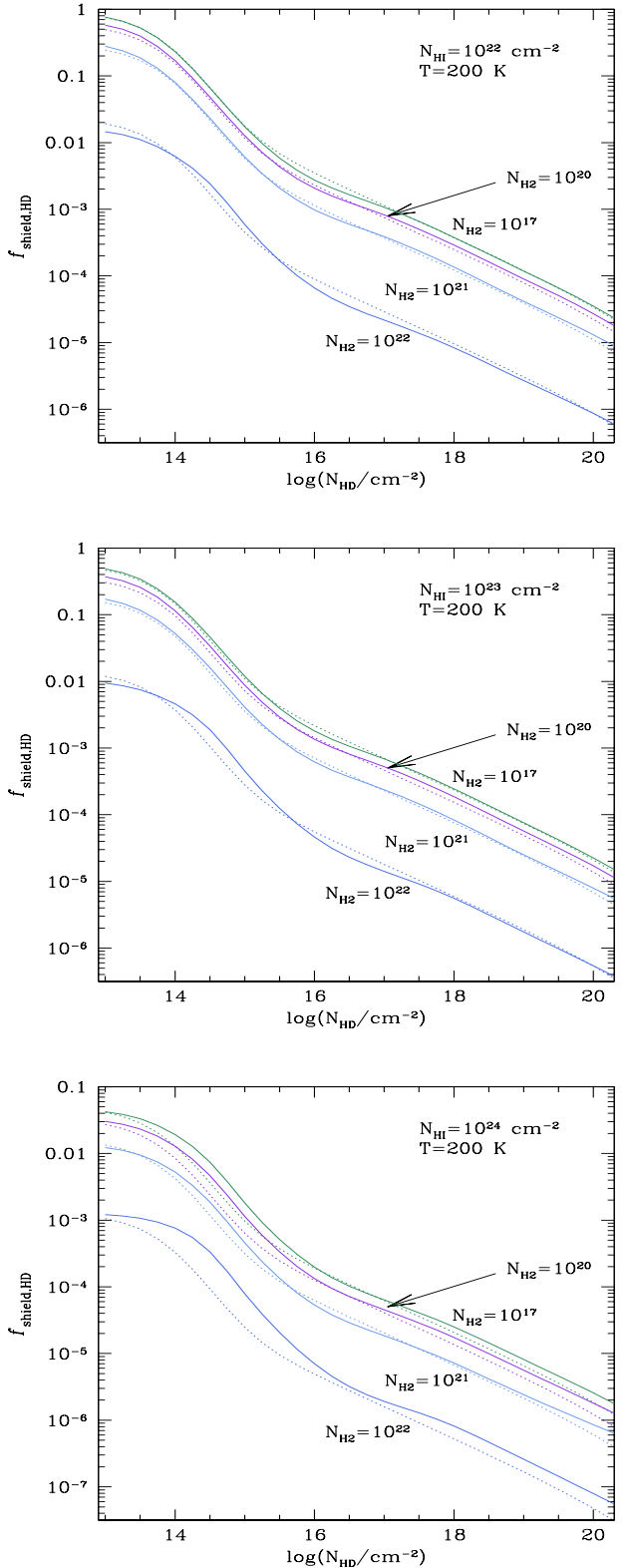


Figure 4. The combined HD shielding factor, including self-shielding and shielding by H_2 and HI. Several combinations of column densities are shown, as labeled, near the critical column densities for HI and H_2 shielding. The solid curves show the exact numerical calculations, and the dotted curves show the values obtained from a fitting formula (equations 8, 11, and 12 and Table 1).

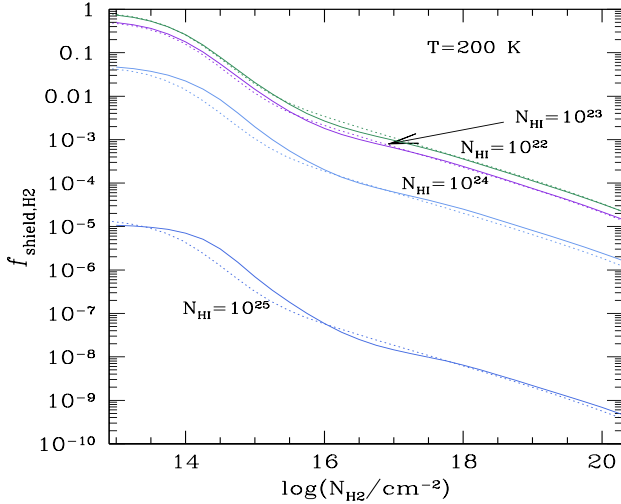


Figure 5. The combined H_2 shielding factor, including self-shielding and shielding by HI. Several combinations of column densities are shown, as labeled, near the critical column densities for HI shielding. The solid curves show the exact numerical calculations, and the dotted curves show the values obtained from a fitting formula (equations 8,12, 13 and Table 1).

similar. At larger neutral hydrogen columns ($N_{\text{HI}} \approx 10^{25}$), a single Lyman H_2 line makes the dominant contribution – by a large margin over all others – to the dissociation rate. Thus, the total shielding factor can again be simply modeled by a product of the shielding formulae, given in equations 8, 12, and Table 1:

$$f_{\text{shield,H}_2} = f_{\text{shield}}(N_{\text{H}_2}, T) \times f_1(N_{\text{HI}}) \quad (13)$$

The results of the exact shielding factor and comparison to this analytical fit are shown in Figure 5 for a gas temperature of $T = 200\text{K}$.

In principle, HD can also shield H_2 , but in practice this effect will likely always be negligible, as the HD column density is typically dwarfed by those of H_2 and HI⁵. Thus, our treatment does not include HD shielding of H_2 .

3 RESULTS

To assess whether HD-cooling can be suppressed by a persistent LW background, we ran our one-zone models at various different specific intensities J_{21} . Unless stated otherwise, the spectrum of the radiation is modeled as a black-body with a temperature of 10^5K , approximating the hard spectrum expected to characterize Pop III.1 stars (Tumlinson & Shull 2000; Bromm et al. 2001; Schaerer 2002). For comparison, in § 3.2.2 below, we investigate the effects of illumination by a cooler blackbody, $T \sim 10^4\text{K}$, intended to represent the softer spectrum of a more typical metal-enriched stellar population. These are referred to hereafter as types ‘T5’ and ‘T4’ respectively (SBH10).

⁵ The fractional abundance of HD relative to that of H_2 could exceed the cosmological D/H ratio by a large factor, owing to chemical fractionation at low temperatures (see, e.g., Galli & Palla 1998). However, it never exceeds $\sim 10^{-2}$ in our models.

We use a Newton-Raphson scheme to determine the strength of the LW radiation required to keep the gas temperature greater than a factor of ~ 2 above that reached in the absence of any LW radiation, $T_{\text{min},J=0}$, on the timescales described below; this is referred to hereafter as the critical intensity: $J_{\text{crit,HD}}$ (in the usual units of $10^{-21}\text{erg cm}^{-2}\text{sr}^{-1}\text{s}^{-1}\text{Hz}^{-1}$).

3.1 HD-Cooling in Constant-Density Fossil HII Gas

The first of the physical scenarios we consider is a “fossil” HII region, which could occur in a patch of the low-density IGM that has been photo-ionized and heated by a short-lived massive star (see, e.g. Oh & Haiman 2003), or possibly in a denser shell of primordial gas, compressed by shocks from a supernova (SN).

We are interested in whether gas with such fossil ionization can cool efficiently in the presence of a LW background and return, via HD cooling, to a state close to its initial low-entropy state, prior to the ignition of the ionizing source (or prior to its shock heating).

In a first set of runs, we assume that the number density remains constant at the low value of $n = 10^{-2}\text{cm}^{-3}$, characteristic of a slightly over-dense (by \sim a factor of 10) region of the IGM at $z = 10$. We find that in such a rarefied patch, the gas is not able to cool on a realistic timescale, because the HD-cooling time is longer than the present age of the universe even in the absence of any LW background. The thermal evolution of the gas in this case is shown by the right set of (purple) curves in the upper panel of Figure 6. The corresponding fractional abundances of electrons, H_2 , and HD are shown in the lower panel of the same figure. The figure extends to a total elapsed time that exceeds the Hubble time, and shows that there is, technically, a critical flux ($J_{\text{crit,HD}} \approx 10^{-6}$) that would suppress the HD-cooling that would otherwise occur after a few $\times 10^{18}$ seconds. This, of course, is unphysical, and in practice, the question of HD-cooling being suppressed by UV radiation is moot for such low-density gas. Nevertheless, the figure illustrates the chemical/thermal behavior, and also provides a useful check on our code (see below).

In the second set of runs, the total particle number density was set to a higher value of $n = 10^2\text{cm}^{-3}$. This is an unphysically high density for a characteristic “flash-ionized” fossil region in the low-density IGM, but may represent primordial gas compressed by SN shocks. In the no-flux case, we reproduce the main result of Johnson & Bromm (2006), namely that HD-cooling allows the gas to reach the temperature of the CMB in a time that is shorter than the Hubble time. This gas, however, is optically thin to radiation in the LW bands, and dissociation of HD (as well as of H_2) is efficient. We find that for $J_{21} \gtrsim 10^{-2}$, the gas cannot cool to temperatures less than $\sim 200\text{K}$. This is shown in the top panel of Figure 6 by the left set of (blue) curves.

The above two cases ($n = 10^{-2}$ and $n = 10^2\text{cm}^{-3}$) serve to illustrate an important point (and a check on our code). All of the relevant timescales for the system, including the formation timescale for HD (t_{form}), the HD cooling time (t_{cool}), and the ($\text{HII}+e \rightarrow \text{HI}$) recombination time (t_{rec}), scale as $1/n$. The exception is the photo-dissociation timescale, which scales with the flux strength, $t_{\text{diss}} \propto J_{21}^{-1}$,

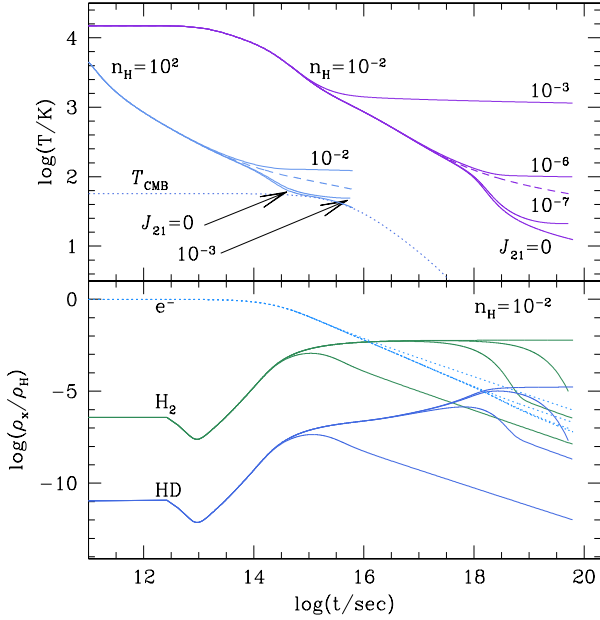


Figure 6. The top panel shows the thermal evolution of constant density gas that is initially fully ionized. The right/left set of solid purple/blue curves adopt densities of 10^{-2} and 10^2 cm^{-3} , appropriate for a flash-ionized patch of the IGM and for primordial gas compressed by a SN-shock, respectively. In both cases, we show the evolution when the gas is exposed to LW backgrounds of various intensities, as labeled. The dashed lines show the temperature reached in deuterium-free gas, in the absence of any LW. The temperature of the CMB, $T_{\text{CMB}} = 2.7(1+z)$, is shown by the dotted blue curve (starting from $z = 20$). The bottom panel shows the fractional abundances of electrons (light blue dotted lines), HD, and H_2 (solid blue and green lines respectively) in the low-density case. The fractional abundances are not shown in the case of the shock-compressed gas for the sake of clarity, and because the patterns they follow are identical to those shown in the lower panel. This figure shows that there is a critical flux, $J_{\text{crit,HD}} = 3.8 \times 10^{-2} (n/10^2 \text{ cm}^{-3})$, that suppresses HD-cooling and prevents the gas from reaching the CMB temperature.

in the absence of shielding. Thus, the history of the system should only depend on J_{21}/n when the time is rescaled accordingly.⁶ This simple scaling is evident by the two sets of (purple and blue) curves in the top panel of Figure 6. Most importantly, there is indeed a critical flux that prevents the gas from reaching the CMB temperature by HD cooling; in constant density gas with a high initial electron fraction, we find the value of this flux is $J_{\text{crit,HD}} = 3.8 \times 10^{-3} (n/10^2 \text{ cm}^{-3})$.

Finally, an interesting question is whether HD-cooling prevented, for the cases in which J_{21} exceeds the critical value, by direct photo-dissociation of HD, or the inability of sufficient HD to form due to H_2 photo-dissociation. To answer this question, we performed runs in which the H_2 -dissociation was artificially turned off. In these runs, we find that the gas is still able to cool to T_{CMB} for

⁶ The interested reader can find a much more detailed discussion of this point for the analogous case of H_2 cooling in Oh & Haiman 2002.

$J_{21} \approx 4 \times 10^{-2}$, illustrating that the LW flux prevents HD-cooling via H_2 destruction, rather than via direct HD-dissociation. This point has been discussed by previous authors, e.g. Nakamura & Umemura (2002) showed that a critical abundance of H_2 , $x_{H_2} \gtrsim 10^{-3}$ is required for the gas to reach sufficiently low temperatures for HD to become the dominant coolant ($T \lesssim 150\text{K}$), and therefore H_2 dissociation can prevent HD-cooling (Yoshida et al. 2007). The minimum temperature reached by fossil ionized primordial gas in the absence of HD, and the dependence of this minimum temperature on gas density and LW flux was also discussed in detail by Oh & Haiman (2003).

3.2 HD Cooling in Collapsing Halos

3.2.1 HD Cooling in Halos with $T_{\text{vir}} > 10^4 \text{ K}$

It has been shown that primordial gas in the late stages of runaway gravitational collapse can reach temperatures close to T_{CMB} via HD-cooling, provided that a large initial ionization fraction exists (e.g. Johnson & Bromm 2006; see also Machida et al. 2005).

This scenario can be realized in sufficiently massive halos, which are collisionally ionized upon shock-heating to their virial temperatures. The post-shock gas can cool faster than it recombines, leaving a large out-of-equilibrium electron fraction to catalyze both H_2 and HD formation (e.g. Shapiro & Kang 1987; Susa et al. 1998; Oh & Haiman 2002). It may also be the case that “pre-ionized” halos exist within fossil HII regions, which will undergo a phase of efficient HD-cooling upon collapse (Johnson & Bromm 2006). This scenario, however, is less plausible: a halo large enough to remain bound once photo-heated (to $T \gtrsim 10^4 \text{ K}$) may be difficult to completely ionize, as the large HI column densities will lead to non-negligible HI self-shielding (Dijkstra et al. 2004); flash-ionization by a single short-lived star (required to allow subsequent recombination and cooling) is even less likely.

Regardless of the nature of the initial ionization, Figure 7 shows the thermal evolution of the collapsing gas exposed to LW backgrounds of various intensities. The initial number density is set to the characteristic baryon density in halos upon virialization,

$$n \simeq 0.3 \text{ cm}^{-3} \left(\frac{1+z_{\text{vir}}}{21} \right)^3, \quad (14)$$

and the gas begins cooling from the temperature $T \approx 10^4 \text{ K}$ (quickly established either by a period of photo-heating, or by shock-heating to near the virial temperature, accompanied by rapid HI cooling).

Of primary importance in this case – as opposed to the fossil gas discussed in the previous section – are the large column densities of HD and H_2 that build up and shield both populations against the LW background. Furthermore, the collapse itself leads to more efficient formation of both molecules because the formation timescale, as mentioned above, scales as $t_{\text{form}} \propto 1/n$. Consequently, the critical intensity should be larger than that found for the low-density fossil gas. This is indeed borne out by our results; nevertheless, as the comparison between the solid and the dashed curves (the latter representing deuterium-free

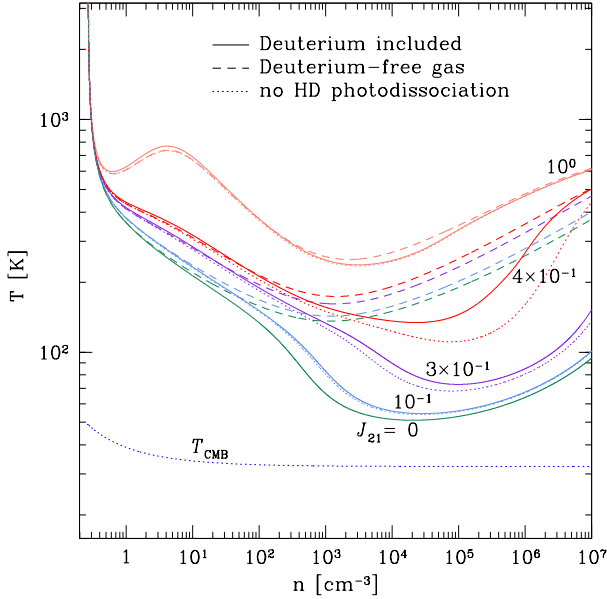


Figure 7. Thermal evolution of initially ionized gas, collapsing in a massive halo ($T_{\text{vir}} \gtrsim 10^4\text{K}$) exposed to LW backgrounds in the range near the critical value, $J_{\text{crit,HD}} = 3.6 \times 10^{-1}$ (solid curves). The incident spectrum is that of a blackbody with a temperature of 10^5K , characteristic of massive Pop III.1 stars. The turnaround redshift is set to $z = 17$ and the temperature is initialized $T \approx 10^4\text{K}$. The dashed curves show, for comparison, the temperature evolution in deuterium-free gas, exposed to the same LW fluxes. The dotted curves show the thermal evolution when HD-dissociation is artificially switched off, for the same values of J_{21} , as labeled. This illustrates that, except in a small range of flux intensities, the destruction of H_2 by LW photons, rather than direct HD photo-dissociation, is the primary factor determining the minimum temperature reached in the gas. The temperature of the CMB is shown by the blue dotted curve.

gas) in Figure 7 shows, the effect of HD-cooling is still almost entirely erased for the relatively low values of $J \gtrsim 1$. The critical intensity in this case, as defined above, is found to be $J_{\text{crit}} = 3.6 \times 10^{-1}$.

This threshold value is most notable for being approximately five orders of magnitude lower than the critical flux required to completely suppress H_2 -cooling in the same halos. As shown in SBH10, the latter critical flux in halos with $T_{\text{vir}} \gtrsim 10^4\text{K}$ is $J_{\text{crit,H}_2} \gtrsim 10^4$. This large critical flux corresponds to the value that results in an H_2 -photo-dissociation rate that matches the H_2 formation rate, at the critical density of $n \sim 10^4\text{cm}^{-3}$ of H_2 (see the earlier work by O01 for a detailed discussion of the physics determining $J_{\text{crit,H}_2}$ in primordial gas without ionization/shock-heating). This $J_{\text{crit,H}_2} \approx 10^4$ separates gas in which H_2 -cooling is *fully* suppressed (with the gas temperature remaining near $\sim 10^4\text{K}$) and halos in which H_2 cooling significantly lowers the temperature. A point that was also found (but not emphasized) by SBH10 (and also by O01) is that even for J_{21} well below $J_{\text{crit,H}_2}$, the minimum temperature to which the gas can cool via H_2 can be significantly elevated. This is also clearly visible in the deuterium-free runs in Figure 7: the mini-

mum temperature is $\sim 150\text{K}$ for $J_{21} = 0$, but is elevated to $\sim 300\text{K}$ already for $J_{21} = 1$.

The behaviour of the gas, and the reason for the elevated temperature, can be described as follows (see a detailed discussion in the constant-density case in Oh & Haiman 2002). Starting from $T \approx 10^4\text{K}$, the gas initially cools via H_2 and recombines on time-scales much shorter than either the photo-dissociation or the free-fall timescale. However, when the temperature is lowered to a J -dependent critical value of a few $\times 10^3\text{K}$, H_2 -dissociation becomes important, limiting the H_2 abundance, and reducing the cooling. The cooling time eventually becomes comparable to the free-fall time, resulting in the sharp turn away from the nearly vertical directions of the $n - T$ curves at the initial density in Figure 7. For higher fluxes, this subsequently results in an elevated gas temperature (at fixed density). Eventually, the compressional heating rate becomes equal to the H_2 -cooling rate, setting the temperature minimum. It is worth noting that for sub-critical values of $J_{21} \lesssim J_{\text{crit,HD}}$, HD is able to cool the gas to temperatures below 150K , but the LW background still has the subtle effect of raising the minimum temperature to which the gas can cool via HD.

As in the constant density case, an interesting question is whether ultimately the HD-cooling is controlled by direct photo-dissociation of HD, or by H_2 -dissociation. To answer this question, we repeated the runs shown in Figure 7 under the same conditions, but with HD dissociation artificially switched off (the results are shown by the dotted lines in Figure 7). In this case, we find again that (except in a narrow range of LW intensities near $J_{21} \sim 4 \times 10^{-1}$), direct photo-dissociation of HD does not determine the minimum temperature reached in the gas. Rather, it is the diminished abundance of H_2 in the presence of the LW background that regulates the abundance and thereby the cooling efficiency of HD.

We have also investigated the thermal evolution of the gas when H_2 is artificially prevented from dissociating (not shown), but the physical set-up is otherwise analogous to the runs (in which deuterium is included) shown in Figure 7. This “academic” exercise is useful in order to determine the critical flux that would prevent HD-cooling entirely by direct HD photo-dissociation. In the analogous case for H_2 , as mentioned above, $J_{\text{crit,H}_2}$ is traditionally defined as the specific intensity capable of *completely* suppressing H_2 -cooling, thereby preventing the gas from falling below the temperatures reached by atomic line cooling, $T \sim 8 \times 10^3\text{K}$ (O01, OSH08, SBH10). We find that for $J \gtrsim 6 \times 10^4$, the cooling history of the gas is nearly identical to that of deuterium-free gas in the absence of a LW background. Thus, the intensity required to fully suppress HD-cooling by direct HD-dissociation is comparable to that of H_2 (the latter was found by the latest studies (SBH10) to be $\sim 1.2 \times 10^4$, but we find a factor of \sim five greater critical value for H_2 ; see below). In fact, this is not surprising, given that the photo-dissociation timescales ($t_{\text{diss}} = [k_{\text{diss}}(N=0) \times f_{\text{shield}}]^{-1}$) are very similar for the two molecules.

3.2.2 $T_{\text{vir}} > 10^4\text{K}$ Halos Illuminated by ‘ T_4 ’ Radiation

Up to this point, we have considered only incident radiation with the hard spectrum expected to characterize Pop III.1

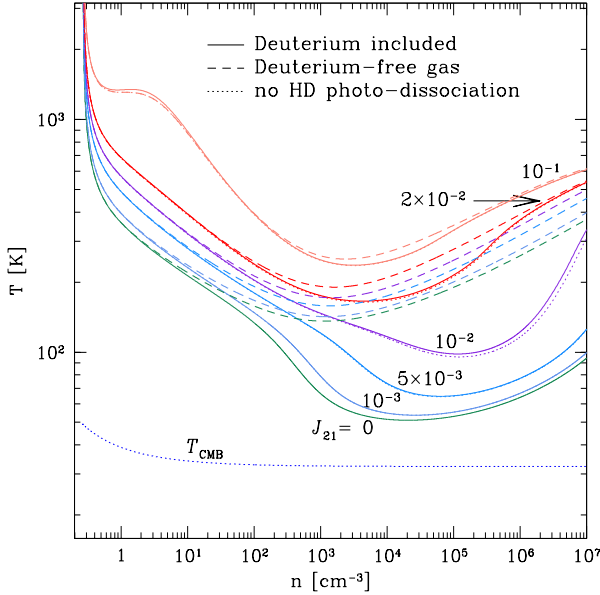


Figure 8. Thermal evolution of gas collapsing in a massive halo, exposed to different LW backgrounds, as in Figure 7, except the incident spectrum is that of a softer blackbody with temperature $T = 10^4$ K, representing a more typical metal-enriched stellar population. This softer spectrum contains many more photons down to the photo-dissociation threshold of H^- at 0.76 eV. The enhanced rate of H^- photo-dissociation reduces the critical flux that prevents HD-cooling by more than an order of magnitude compared to the harder spectrum, to $J_{\text{crit,HD}} = 10^{-2}$.

stars (‘T5’). In the case of a collapsing halo, it is reasonable to ask about the effects of irradiation by the more typical stellar spectrum (‘T4’), on HD-cooling.

Figure 8 shows the temperature evolution in the gas irradiated by a T4 spectrum of various intensities. It is clear that HD is considerably more fragile in the presence of this softer spectrum, withstanding a LW flux no greater than a feeble $J_{\text{crit,HD}} = 10^{-2}$. This is not surprising in the light of studies that have found the same effect for H_2 (O01; OSH08; SBH10), namely, that H_2 -cooling is much more effectively suppressed by the T4 type spectrum. The reason is the diminished abundance of hydride (H^-), an intermediary in the formation of both H_2 and HD. Hydride, whose ionization threshold is 0.76 eV, is more efficiently photo-dissociated by the softer spectral type (O01, SBH10). This again is a manifestation of how an external radiation field can regulate HD-cooling *via* the destruction of an intermediate in its formation pathway.

3.2.3 HD Cooling in $T_{\text{vir}} < 10^4$ K Halos

It has long been known that pristine gas in the first mini-halos cannot form sufficient H_2 to cool below a few hundred Kelvin (e.g. Haiman et al. 1996). Because free electrons act to catalyze the formation of HD, as well as H_2 , it is not surprising that HD abundances remain too low in such halos to play a significant role in cooling (e.g. Johnson & Bromm 2006, and references therein). This is borne out by our re-

sults, shown in Figure 9, for a halo that begins collapsing from a temperature of $T \approx 20$ K at the turnaround redshift, $z = 17$, and is illuminated by a ‘T5’ spectrum. This is the same configuration as in Figure 7, except that the initial temperature is assumed to be low (i.e., lacking any strong shocks able to collisionally excite or ionize the gas).

We include a discussion of this scenario for the purpose of highlighting a few noteworthy points. First, we find a critical flux for full H_2 -dissociation in this case (as it is traditionally defined, see § 3.2.1 above) of $J_{\text{crit,H}_2} = 6.1 \times 10^4$, which is a factor of \sim five greater than that found in the recent study by SBH10. This difference owes to our use of the analytic fit for H_2 self-shielding (equation 8), which assumes all molecules are initially the ground state, while SBH10 used the shield factor fit (equation 36) from DB96, which gives a very good approximation to the self-shielding when the H_2 ro-vibrational levels reach LTE populations. This illustrates an important point that will be discussed in greater depth in § 4; namely, self-shielding is *less* effective when higher ro-vibrational states of the molecule are populated (see more discussion in § 4 below). It is also worth noting that we find $J_{\text{crit,H}_2} = 6 \times 10^3$ – a factor of 2 *lower* than that found by SBH10 – if the self-shielding is modeled instead with the more accurate formula provided by DB96 (equation 37), rather than the power-law fit (equation 36) used by SBH10. In general, the “real” LW intensity required to kill H_2 -cooling entirely will depend on the detailed ro-vibrational distribution of H_2 molecules. The values of $J_{\text{crit,H}_2}$ found here using the ground-state *vs* LTE shielding treatments serve to bracket the range for the true critical threshold, with the former approximating the upper limit on $J_{\text{crit,H}_2}$. The threshold flux in this case is of particular interest as it has important implications for the number of halos that remain H_2 -poor, and thus for the abundance of halos collapsing directly to massive seed black holes, because such halos probe the rare, exponential tail of the fluctuating UV background (Dijkstra et al. 2008). (The interested reader is encouraged to see SBH10 for a detailed discussion of these issues.)

Second, while there is a clear bifurcation in the cooling history of the gas around the $J_{\text{crit,H}_2}$ discussed above, we note that it does not cool to the low temperatures required for HD-cooling to become important ($T \sim 150$ K) even when the intensity is well below this threshold (indeed, even in the absence of any LW background). Thus, again, H_2 abundance plays the primary role in regulating HD-cooling, though in this case the result is simpler: HD-cooling never becomes important because H_2 -cooling is never strong enough for the gas temperature to fall below ≈ 200 K.

Finally, in this case HI shielding serves to increase the threshold LW flux by $\sim 40\%$ above that which H_2 could otherwise withstand. By contrast, $J_{\text{crit,HD}}$ found in the two preceding sections is not sensitive to the effect of H_2 shielding by HI, in spite of its strong dependence on the H_2 abundance. This is because, in the models of $T_{\text{vir}} \gtrsim 10^4$ K halos, the HI column density does not reach the critical value above which it effectively shields H_2 ($N_{\text{HI}} \gtrsim 10^{23} \text{ cm}^{-2}$) until very late in the collapse (i.e., once the particle density has reached $n \gtrsim 10^{5.5} \text{ cm}^{-3}$). However, sufficiently high column densities of HI do build up earlier in the high- J_{21} runs of $T_{\text{vir}} < 10^4$ K halos, resulting in the modest increase in $J_{\text{crit,H}_2}$ as quoted above.

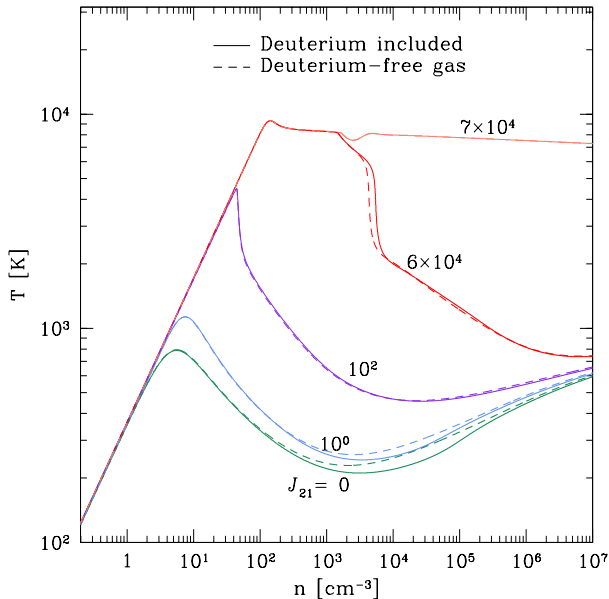


Figure 9. Thermal evolution of gas collapsing in a halo exposed to LW radiation (with a T5 spectrum) in Figure 7, except that the initial gas temperature is assumed to be much lower, 21K. This is relevant to minihalos ($T_{\text{vir}} \lesssim 10^4\text{K}$), or to the case when there are no strong shocks able to collisionally excite or ionize the gas.

The results for the halo illuminated by a T4 spectrum are omitted here because they do not significantly differ from those described above for the T5 case, except that H_2 -cooling is disabled by a much lower LW flux, as shown already by O01.

4 DISCUSSION

The most significant result found in this paper is that a UV flux can prevent HD-cooling from lowering the gas temperature to near that of the CMB. In particular the threshold value in collapsing halos, $J_{\text{crit,HD}} \sim 4 \times 10^{-1}$, is approximately five orders of magnitude lower than the critical flux required to completely suppress H_2 -cooling in the same halos. As explained in § 3.2.1, this large difference arises because even for J_{21} well below $J_{\text{crit,H}_2}$, the minimum temperature to which the gas can cool via H_2 is significantly elevated, so that HD formation and cooling is not activated. *What are the cosmological implications if a LW background prevents halos from cooling via HD line emission?* The critical flux we find should be compared to the level of the LW background J_{bg} expected at the redshifts we consider. For reference, an estimate of the background as a function of redshift is provided by requiring the number of UV photons produced by stars to be sufficient to reionize the IGM. Such an estimate gives (e.g. Bromm & Loeb 2003)

$$J_{\text{bg}} \approx 4 \left(\frac{N_\gamma}{10} \right) \left(\frac{f_{\text{esc}}}{100\%} \right)^{-1} \left(\frac{1+z}{11} \right)^3. \quad (15)$$

Here the number of UV photons required to ionize hydrogen is commonly taken to be $N_\gamma \sim 10$, and the escape frac-

tion f_{esc} is the fraction of ionizing photons (13.6eV) escaping from galaxies at high redshifts, which is expected to be close to unity (Whalen et al. 2004; see Fernandez & Shull 2010 for a recent discussion of the relevant f_{esc} and for references to earlier works). From this equation, we find that the mean UV background at the time of reionization exceeds the critical flux $J_{\text{crit,HD}}$ by nearly an order of magnitude. While the radiation background will inevitably have spatial fluctuations, this implies that most halos collapsing in the early IGM, prior to reionization at $z \sim 10-20$, would be exposed to a super-critical flux and thus not able to cool below $T \sim 200\text{K}$. As a result, the emergence of low-mass PopIII.2 stars (or stars comparable in mass to those formed in the low-redshift universe) would be postponed until supernovae polluted the IGM with heavy elements, and metal-line cooling subsequently enabled gas clouds to reach temperatures near T_{CMB} .

There are several issues that could be important for the above conclusion, which we have glossed over in the discussion of our models for molecular shielding and one-zone spherical collapse. We next discuss some of these.

Uncertainty in the Column Density of the Collapsing Region. In our calculations, we have taken the diameter of the collapsing region to be of the order of the Jeans length. However, the effective size and column density will depend sensitively on the dynamical properties of the system, including bulk motions and internal velocity gradients in the gas, departures from spherical symmetry, etc.

In order to address this uncertainty quantitatively, we have performed two additional sets of runs for a halo with $T_{\text{vir}} \gtrsim 10^4\text{K}$ (analogous to those in § 3.2.1). In the first, we increase the assumed size of the collapsing region by a factor of ten (i.e. to ten times the Jeans length λ_J). This increases the column densities by the same factor, and accordingly, J_{crit} is larger by a factor of ~ 3 than the original result, due to more efficient self-shielding of H_2 and – to a lesser extent – HD. Next, we investigated the cooling properties of a smaller collapsing core, with the assumed size reduced by a factor of ten, to $0.1\lambda_J$. In this case, a new effect arises. Namely, for the values of J_{21} at which the gas can (just) cool to around $T \sim 200\text{K}$, we find that direct HD dissociation is the dominant factor regulating the minimum temperature ultimately reached. In particular, switching HD dissociation off by hand in these cases decreases the gas temperature by a factor of ~ 1.5 at high number densities ($n \gtrsim 10^4 \text{ cm}^{-3}$) for $J = 10^{-1}$. When the flux is weaker than this, artificially disabling the HD-dissociation has little effect; for these low fluxes, however, the suppression of HD-cooling is modest to begin with. As expected, the critical flux is decreased in this case because the smaller column densities leave both H_2 and HD more susceptible to dissociation. In particular, we find a critical value of $J_{\text{crit}} \sim 10^{-1}$.

The Impact of 3-D Gas Dynamics on Self-Shielding. It is important to note that a full treatment of the three-dimensional dynamics of the system and the complexities inherent in radiative transfer is needed to solve the shielding problem exactly. Our calculation is based on a model of a uniform slab of gas with no internal velocity (or temperature) gradients. This is likely to be a poor approximation for a region undergoing runaway gravitational collapse, in which high gas velocities can produce significant Doppler shifts of the LW absorption bands of H_2 and HD. In general, we expect this to

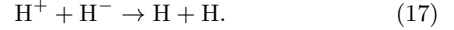
reduce the effective column densities, and the importance of shielding, compared to our calculations. This correction can be mitigated by the broadening of absorption lines at high column densities, which leads to line widths that are much larger than the average Doppler shift. In general, however, taking into account the possibility of Doppler shifts leads to the conclusion that our self-shielding results, and in turn the values quoted for $J_{\text{crit,HD}}$, are *upper limits* for both. This strengthens our argument above, namely, that most collapsing halos will see a super-critical flux.

Resonant Scattering of Incident LW Photons. An additional effect ignored by our self-shielding calculation is that after absorbing a LW photon, a fraction of molecules will decay directly back to the original ground state, as opposed to cascading through a series of lower energy decays as we implicitly assume. These photons are thus not eliminated, making the background flux stronger than we calculate. However, Glover & Brand (2001) estimate that in the case of H_2 , such resonant scattering constitutes only a small fraction, 4–8%, of all LW absorption events (depending on the initial level populations; in particular, on the ortho/para ratio). Hence this is a minor effect, which again makes our conclusions about the suppression of HD-cooling conservative.

Molecular Level Populations: Implications for Photo-dissociation Rates and the Critical Flux. As described in §2.3, our fiducial self-shielding calculations for HD and H_2 assume that all molecules are initially in the ro-vibrational and electronic ground states. In reality, molecules will occupy higher ro-vibrational states due to collisional excitation, and this can significantly *increase* the rates of photo-dissociation. In particular, we find that self-shielding is less effective (i.e. the shield factor is larger by a factor of a \sim few) if we repeat our calculations, assuming LTE population distributions in the rotational levels ($J \neq 0$) within the ground electronic and vibrational state. (Data for the HD and H_2 energy levels were taken from Abgrall et al. 1982 and Dabrowski 1984 respectively.) Other studies have also noted that populations in higher vibrational levels ($v \neq 0$) can significantly increase the rates of photo-dissociation (e.g. Glover & Jappsen 2007, and references therein). Thus, if the effects of collisional excitation are taken into account, $J_{\text{crit,HD}/\text{H}_2}$ could be significantly lower than found above. The ro-vibrational distribution will be somewhat better approximated by the ground state model up to the critical densities ($n \gtrsim 10^4 \text{ cm}^{-3}$ for H_2 and $n \gtrsim 10^6 \text{ cm}^{-3}$ for HD). In our case, the fate of the collapsing clouds – whether it will ultimately cool to temperatures low enough for HD-cooling to become significant – is determined in the regime of somewhat lower gas densities, below those at which equilibrium H_2 populations are established, so that J_{crit} values are likely closer to the upper end of the range.

Uncertainties in the Gas Phase Chemistry. The preceding discussion has focused on various uncertainties associated with photo-dissociation rates of H_2 and HD; however, the accuracy of any estimates of $J_{\text{crit,HD}}$ can only be as good as the accuracy of the underlying chemical rate coefficients. Considerable attention has been dedicated to uncertainties in both H_2 and HD chemistry and cooling, (e.g. Savin et al. 2004, Glover et al. 2006, Glover 2008, Glover & Abel 2008); accordingly, we restrict the discussion here to focus on two examples of thermal rate coefficients that have recently been updated, and how their revised values affect our results.

Two reaction rates that are crucial for determining the abundance of H_2 , particularly in gas with a large initial ionization fraction, have been estimated to be uncertain by up to an order of magnitude (e.g. Glover & Abel 2008). These are the associative detachment channel for H_2 formation, and the mutual neutralization of hydride and protons (reactions 10 and 13 respectively in the compilation by SBH10):



Both have been revisited recently and new thermal rate coefficients have been provided for reaction (10) by Kreckel et al. (2010) and for reaction (13) by Stenrup et al. (2009). As noted above, the formation of HD occurs primarily via the reaction pathway shown in equations 1–3, so in general, the fractional abundance of HD is proportional to that of H_2 , justifying the emphasis here on uncertainties associated with the formation of H_2 . In order to quantify how these recently updated rate coefficients impact our results, we have performed additional runs for each of the physical scenarios discussed in §3. The uncertainties these introduce into estimates of $J_{\text{crit,HD}}$ and the minimum temperature, T_{min} , reached when $J_{21} = 0$, are summarized below.

We examine three published rate coefficients for the mutual neutralization reaction; the largest of these at all temperatures is that provided by GP98, hereafter k_{13b} . The rate used in our fiducial model (k_{13}), originally provided by Dalgarno & Lepp (1987), is smaller than the others by up to \sim an order of magnitude for $T \gtrsim 10^3 \text{ K}$, and by a factor of several at lower temperatures.⁷ The value of the newest thermal rate coefficient, given by Stenrup et al. (2009), k_{13c} , lies between those of k_{13} and k_{13b} at all temperatures in the regime we study. Using k_{13b} , we find the critical flux, $J_{\text{crit,HD}}$ is a factor of ~ 2 lower than was found in each of the physical scenarios we have studied (see §3; note that this does not apply to the model of halos with $T_{\text{vir}} < 10^4 \text{ K}$), and T_{min} is $\sim 30\%$ greater in the spherical collapse models. This is easily explained: when a large ionization fraction exists, reaction (13) competes with reaction (10) for the common reactant, H^- ; thus, adopting a larger rate coefficient for reaction (13) leads to diminished abundance of, and less robust cooling by H_2 . Using the newest rate, k_{13c} , we find the critical flux is $\sim 30 - 40\%$ smaller than its original value for each physical scenario, and the minimum temperature is elevated $\sim 20\%$ above that found previously in the spherical collapse models. (Note that the minimum temperature reached in the fossil HII region models does not depend on which rate coefficient is used for reaction 13.)

The effect of implementing the new rate for associative detachment is less dramatic; note, however, that the uncertainty associated with this rate coefficient has been reduced thanks to the recent study by Kreckel et al. (2010). Using the systematic uncertainty given by the authors, we implement the thermal rate at the $\pm 1\sigma$ levels, and find the following ranges for the critical flux. In the fossil HII region:

⁷ Glover et al. (2006) have suggested that this rate is in fact erroneously small, perhaps due to typographical errors in the source. Nonetheless, it is widely used in studies of star formation in metal-free gas.

$J_{\text{crit,HD}} = 3.85 \pm 0.15 \times 10^{-3} [n/10^2]$. In $T_{\text{vir}} > 10^4 \text{ K}$ halos: $J_{\text{crit,HD}} = 3.7 \pm 0.2 \times 10^{-1}$ and $1.2 \pm 0.3 \times 10^{-2}$ when illuminated by T5 and T4 spectral types respectively. For a thorough discussion of how this new rate coefficient compares to previous calculations and its impact on H_2 chemistry, the reader is referred to Kreckel et al. (2010).

Two final notes on the chemical network are on order: first, we have not included in this study the formation of H_2 via a three-body reaction, by which metal-free gas can become fully molecular at $n \gtrsim 10^8 \text{ cm}^{-3}$, because our models do not include these high-density regimes. Lastly, as mentioned above, the primordial value of D/H varies in the literature by a factor of ~ 2 , and this in itself may have consequences for the role of HD-cooling in metal-free gas.

Fragmentation and Characteristic Protostellar Masses. Finally, we emphasize that all our conclusions in this paper are based on the thermal history of a gas cloud, and how this is affected by a UV flux. In order to make realistic predictions for the fragmentation, and the ultimate sizes of stars forming in a collapsing halo, fully 3-D hydrodynamical simulations would be required. While robust HD-line cooling (or lack thereof) could have a notable impact on the characteristic stellar masses in the earliest dwarf galaxies, the process of fragmentation is yet to be fully understood, and thus physical ingredients such as the minimum gas temperature may not directly translate into the actual mass of the protostar that ultimately forms (see, e.g., Clark et al. 2010 for recent results on fragmentation in metal-free gas, and in particular the importance of turbulence).

5 SUMMARY

We have demonstrated that HD-cooling in primordial gas can be suppressed by a relatively weak external LW background, with an intensity on the order of $J_{21} \sim 10^{-3} (n/10^{-2} \text{ cm}^{-3})$ in constant-density “fossil ionized” gas, and $J_{21} \sim 10^{-1}$ in shock- or photo-ionized gas collapsing into halos with virial temperatures greater than $\sim 10^4 \text{ K}$. These critical intensities are lower than the expected mean UV background at $z \sim 10 - 20$, suggesting that HD-cooling is likely unimportant in most proto-galaxies forming near and just prior to the epoch of reionization. We conclude that an “HD-mode” of star formation was not as prevalent as previously thought.

On a more technical note: we have also found that the negative feedback of the LW background is mediated via the abundance of molecular hydrogen, which is dissociated by the same radiation in its Lyman and Werner bands. Direct HD photo-dissociation is comparatively less important, although we find that in regimes of less effective self-shielding, it can regulate the minimum temperature of the gas. Finally, we have provided fitting formulae for the effects of HD and H_2 self-shielding, shielding of both species by HI, and shielding of HD by H_2 , which we hope will be useful in other future studies.

6 ACKNOWLEDGMENTS

We would like to thank Volker Bromm, Greg Bryan, Simon Glover and Daniel Savin for useful discussions. This work

was supported by the Polányi Program of the Hungarian National Office for Research and Technology (NKTH).

REFERENCES

- Abel T., Bryan G. L., Norman M. L., 2002, *Science*, 295, 93
- Abgrall H., Roueff E., 2006, *A&A*, 445, 361
- Abgrall H., Roueff E., Drira I., 2000, *A&AS*, 141, 297
- Abgrall H., Roueff E., Launay F., Roncin J. Y., Subtil J. L., 1993a, *A&AS*, 101, 273
- Abgrall H., Roueff E., Launay F., Roncin J. Y., Subtil J. L., 1993b, *A&AS*, 101, 323
- Abgrall H., Roueff E., Viala Y., 1982, *A&AS*, 50, 505
- Bromm V., Coppi P. S., Larson R. B., 2002, *ApJ*, 564, 23
- Bromm V., Kudritzki R. P., Loeb A., 2001, *ApJ*, 552, 464
- Bromm V., Loeb A., 2003, *ApJ*, 596, 34
- Bromm V., Yoshida N., Hernquist L., McKee C. F., 2009, *Nature*, 459, 49
- Clark P. C., Glover S. C. O., Klessen R. S., Bromm V., 2010, *ApJ*, submitted, e-print arxiv:1006.1508
- Dabrowski I., 1984, *Canadian Journal of Physics*, 62, 1639
- Dalgarno A., Lepp S., 1987, in M. S. Vardya & S. P. Tarafdar ed., *Astrochemistry Vol. 120 of IAU Symposium, Chemistry in the early universe*. pp 109–118
- Dijkstra M., Haiman Z., Mesinger A., Wyithe J. S. B., 2008, *MNRAS*, 391, 1961
- Dijkstra M., Haiman Z., Rees M. J., Weinberg D. H., 2004, *ApJ*, 601, 666
- Draine B. T., Bertoldi F., 1996, *ApJ*, 468, 269
- Fernandez E. R., Shull J. M., 2010, *ApJ*, submitted, e-print arXiv:1006.3519
- Galli D., Palla F., 1998, *A&A*, 335, 403
- Galli D., Palla F., 2002, *planss*, 50, 1197
- Glover S., 2008, in B. W. O’Shea & A. Heger ed., *First Stars III Vol. 990 of American Institute of Physics Conference Series, Chemistry and Cooling in Metal-Free and Metal-Poor Gas*. pp 25–29
- Glover S. C., Savin D. W., Jappsen A., 2006, *ApJ*, 640, 553
- Glover S. C. O., Abel T., 2008, *MNRAS*, 388, 1627
- Glover S. C. O., Brand P. W. J. L., 2001, *MNRAS*, 321, 385
- Glover S. C. O., Jappsen A., 2007, *ApJ*, 666, 1
- Glover S. C. O., Savin D. W., 2009, *MNRAS*, 393, 911
- Haiman Z., Rees M. J., Loeb A., 1996, *ApJ*, 467, 522
- Haiman Z., Rees M. J., Loeb A., 1997, *ApJ*, 484, 985
- Haiman Z., Thoul A. A., Loeb A., 1996, *ApJ*, 464, 523
- Johnson J. L., Bromm V., 2006, *MNRAS*, 366, 247
- Kirkman D., Tytler D., Suzuki N., O’Meara J. M., Lubin D., 2003, *ApJS*, 149, 1
- Komatsu E., Dunkley J., Nolte M. R., Bennett C. L., B. G., Hinshaw G., Jarosik N., Larson D., Limon M., Page L., Spergel D. N., Halpern M., Hill R. S., Kogut A., Meyer S. S., Tucker G. S., Weiland J. L., Wollack E., Wright E. L., 2009, *ApJS*, 180, 330
- Kreckel H., Bruhns H., Čížek M., Glover S. C. O., Miller K. A., Urbain X., Savin D. W., 2010, *Science*, 329, 69
- Lipovka A., Núñez-López R., Avila-Reese V., 2005, *MNRAS*, 361, 850
- Machida M. N., Tomisaka K., Nakamura F., Fujimoto M. Y., 2005, *ApJ*, 622, 39

- McGreer I. D., Bryan G. L., 2008, *ApJ*, 685, 8
 Nagakura T., Omukai K., 2005, *MNRAS*, 364, 1378
 Nakamura F., Umemura M., 2002, *ApJ*, 569, 549
 Oh S. P., Haiman Z., 2002, *ApJ*, 569, 558
 Oh S. P., Haiman Z., 2003, *MNRAS*, 346, 456
 O’Meara J. M., Burles S., Prochaska J. X., Prochter G. E.,
 Bernstein R. A., Burgess K. M., 2006, *ApJL*, 649, L61
 Omukai K., Schneider R., Haiman Z., 2008, *ApJ*, 686, 801
 Ripamonti E., 2007, *MNRAS*, 376, 709
 Savin D. W., 2002, *ApJ*, 566, 599
 Savin D. W., Krstić P. S., Haiman Z., Stancil P. C., 2004,
ApJL, 606, L167
 Schaerer D., 2002, *A&A*, 382, 28
 Shang C., Bryan G. L., Haiman Z., 2010, *MNRAS*, 402,
 1249
 Shapiro P. R., Kang H., 1987, *ApJ*, 318, 32
 Stenrup M., Larson A., Elander N., 2009, *Phys. Rev. A*,
 79, 012713
 Susa H., Uehara H., Nishi R., Yamada M., 1998, *Progress*
of Theoretical Physics, 100, 63
 Tumlinson J., Shull J. M., 2000, *ApJL*, 528, L65
 Whalen D., Abel T., Norman M. L., 2004, *ApJ*, 610, 14
 Yoshida N., Oh S. P., Kitayama T., Hernquist L., 2007,
ApJ, 663, 687
 Yoshida N., Omukai K., Hernquist L., 2007, *ApJL*, 667,
 L117

